

Reactivity of Novel *N,N'*-Diphosphino-Silanediamine-Based Rhodium(I) Derivatives

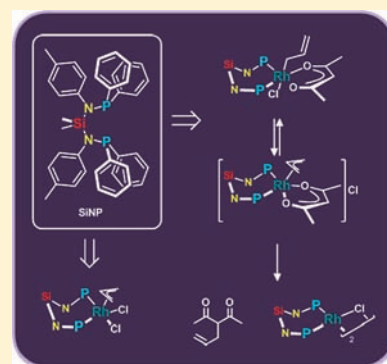
Vincenzo Passarelli*[†] and Franco Benetollo[‡]

[†]Centro Universitario de la Defensa, Ctra. Huesca s/n, ES-50090 Zaragoza, España

[‡]Instituto di Chimica Inorganica e delle Superfici (ICIS), Consiglio Nazionale delle Ricerche, Corso Stati Uniti 4, I-35127 Padova, Italia

S Supporting Information

ABSTRACT: The coordination abilities of the novel *N,N'*-diphosphino-silanediamine ligand of formula $\text{SiMe}_2(\text{NtolPPh}_2)_2$ (SiNP, **1**) have been investigated toward rhodium, and the derivatives $[\text{RhCl}(\text{SiNP})]_2$ (**2**), $[\text{Rh}(\text{SiNP})(\text{COD})][\text{BF}_4]$ (**3**), and $\text{Rh}(\text{acac})(\text{SiNP})$ (**4**) have been synthesized. The stability of the dinuclear frame of $[\text{RhCl}(\text{SiNP})]_2$ (**2**) toward incoming nucleophiles has been shown to be dependent on their π -acceptor ability. Indeed, the mononuclear complexes $\text{RhCl}(\text{SiNP})(\text{L})$ ($\text{L} = \text{CO}$, **5**; CN^tBu , **6**) have been isolated purely and quantitatively upon reaction of **2** with CO and CN^tBu , respectively. Otherwise, PPh_3 and $\text{RhCl}(\text{SiNP})$ equilibrate with $\text{Rh}(\text{Cl})(\text{SiNP})(\text{PPh}_3)$ (**7**). Carbon electrophiles such as MeI and 3-chloro-1-propene afforded the oxidation of rhodium(I) to rhodium(III) and the formation of $\text{RhCl}_2(\eta^3\text{-C}_3\text{H}_5)(\text{SiNP})$ (**8**) and $\text{Rh}(\text{Me})(\text{I})(\text{SiNP})(\text{acac})$ (**10**), respectively. The methyl derivative **10** is thermally stable and does not react either with CO or with CN^tBu even in excess. Otherwise, $\text{RhCl}_2(\eta^3\text{-C}_3\text{H}_5)(\text{SiNP})$ (**8**) is thermally stable but reacts with CO, affording 3-chloro-1-propene and $\text{RhCl}(\text{SiNP})(\text{CO})$ (**5**). Finally, upon reaction of $\text{Rh}(\text{acac})(\text{SiNP})$ (**4**) and 3-chloro-1-propene, $\text{RhCl}(\text{acac})(\eta^1\text{-C}_3\text{H}_5)(\text{SiNP})$ (**9a**) and $[\text{Rh}(\text{acac})(\eta^3\text{-C}_3\text{H}_5)(\text{SiNP})]\text{Cl}$ (**9b**) could be detected at 233 K. At higher temperatures, **9a** and **9b** smoothly decompose, affording the dinuclear derivative $[\text{RhCl}(\text{SiNP})]_2$ (**2**) and the CC coupling product 3-allylpentane-2,4-dione.



INTRODUCTION

The rational design of novel ligands or the structural modification of known ones, either at the donor atoms or of their overall structure, is a basic strategy used to modulate the reactivity of metal complexes. Indeed, the change in the electronic and/or steric properties of the donor atoms as well as of the ligand itself can induce a tailored reactivity at the coordinated metal center. Relevant to this paper, ligands containing P–N bonds have shown great versatility in both organometallic chemistry and catalysis,¹ and a few years ago, Woolins and co-workers reported^{2,3} the stepwise synthesis of $\text{SiMe}_2[(\text{C}_5\text{H}_4\text{N}-2)\text{-NPPH}_2]_2$ (from now onward SiN^{PYP} , Scheme 1A) *via* the aminolysis of the $\text{Ph}_2\text{P}-\text{Cl}$ bond by 2-aminopyridine, NH deprotonation of the resulting phosphinoamine $(\text{C}_5\text{H}_4\text{N}-2)\text{NHPPH}_2$, and final chloride substitution in SiMe_2Cl_2 (Scheme 1A). Also, the palladium and platinum complexes of formula $\text{MX}_2(\text{SiN}^{\text{PYP}})$ ($\text{X} = \text{Cl}, \text{Me}$) were reported along with the observation³ that the reaction of SiN^{PYP} with $[\text{RhCl}(\text{COD})]_2$ or $[\text{RhCp}^*\text{Cl}_2]_2$ results in the hydrolysis of the Si–N bond (Scheme 1A) probably due to adventitious water.

On the other hand, a survey of the literature showed that, besides the above-mentioned $\text{MX}_2(\text{SiN}^{\text{PYP}})$ ($\text{M} = \text{Pd}, \text{Pt}$; $\text{X} = \text{Cl}, \text{Me}$), very few further examples⁴ (namely with Ni, Pd, Pt, Mo, and W, Scheme 1B) are reported, in which a transition metal is bonded to a P–N–Si–N–P scaffold.

Thus, provided that (a) diphosphines are versatile ligands extensively used in order to both stabilize transition metals and

promote their catalytic activity^{5,6} and (b) the reported route to SiN^{PYP} suggests that, in principle, the appropriate choice of the starting materials could allow easy incorporation in the P–N–Si–N–P frame of a great variety of substituents (both at silicon, nitrogen, and/or phosphorus), we decided to contribute to the so far barely explored chemistry of the *N,N'*-diphosphino-silanediamines by preparing a new ligand of this family and investigating its interaction with rhodium as well as the reactivity of the newly prepared complexes.

RESULTS AND DISCUSSION

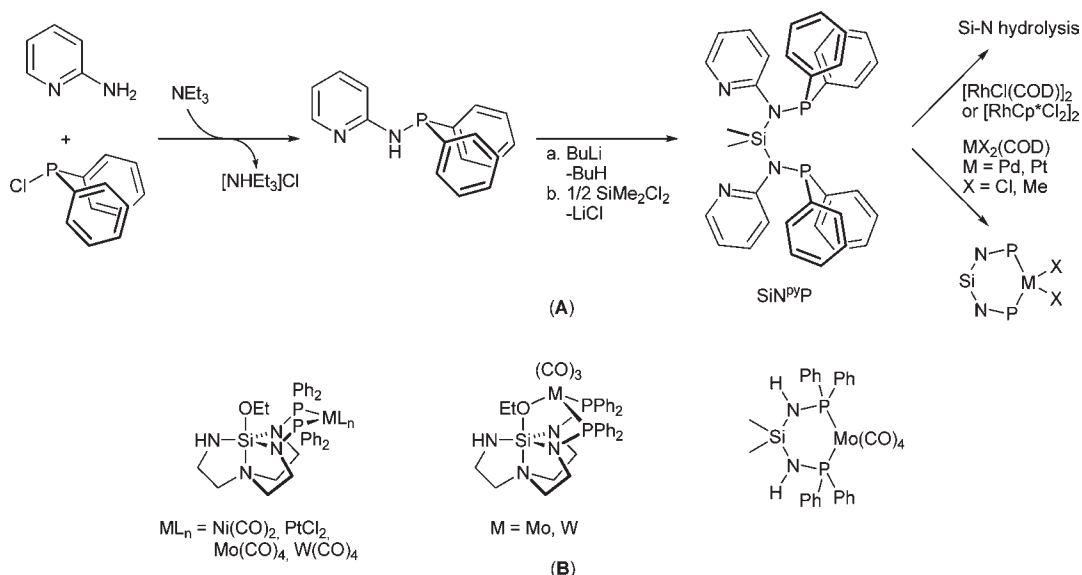
The ligand *N,N'*-bis(diphenylphosphino)-1,1-dimethyl-*N,N'*-di-*p*-tolyl-silanediamine $\text{SiMe}_2(\text{NtolPPh}_2)_2$ (SiNP, **1**) is cleanly obtained by the two-step synthesis reported in Scheme 2: 1,1-diphenyl-*N*-(*p*-tolyl)phosphinoamine (NHtolPPh_2 , **A**) is prepared purely and with high yields through the reaction of NH_2tol with PClPh_2 (2:1 molar ratio); the deprotonation of **A** by $^t\text{BuLi}$ and the following reaction with SiMe_2Cl_2 yields SiNP (**1**) as a pure microcrystalline colorless solid (Scheme 2). Relevant NMR data for **1** are reported in Table 1.

SiNP is thermally stable toward O_2 ; indeed oxidation was not observed even after prolonged (up to 2 days) exposure to O_2 (either atmospheric or pure), both in toluene solution or in the

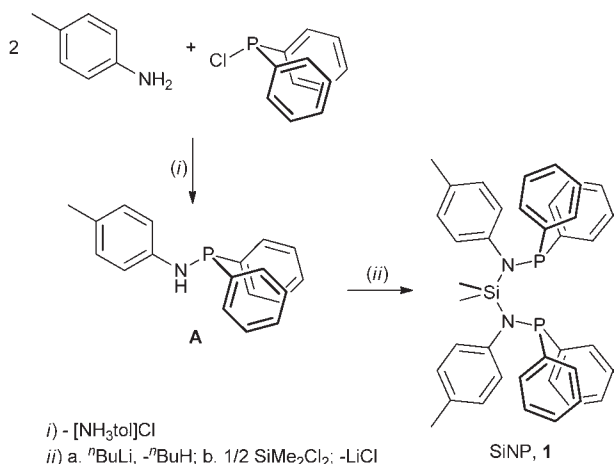
Received: March 4, 2011

Published: September 22, 2011

Scheme 1



Scheme 2



solid state, and eventually heating at 80 °C. On the other hand, water may afford the hydrolysis of the Si–N bond, but heat and a large excess of water are necessary (water/acetone 50%_{v/v}, 70 °C, 6 h) in order to observe approximately 40% conversion of **1** to NHtolPPh₂ and uncharacterized silane derivatives.

A family of square planar rhodium(I) complexes is obtained by the reaction of SiNP with classical rhodium(I) precursors (Scheme 3). Indeed, acetonitrile in [Rh(COD)(MeCN)₂]⁺ is readily displaced by SiNP, affording the cationic mononuclear complex [Rh(SiNP)(COD)]⁺ (**3**). In a similar way, CO and COD are substituted in Rh(acac)(CO)₂ and [RhCl(COD)]₂, respectively, affording the bis-chelate complex Rh(acac)(SiNP) (**4**) and the chloro-bridged derivative [RhCl(SiNP)]₂ (**2**) (Scheme 3).

Relevant NMR data for the compounds **2**–**4** are given in Table 1. In general, the coordination of SiNP to rhodium(I) causes the downfield shift of its ³¹P signal, and the observed ¹J_{PRh} coupling constants are in the range typical of rhodium(I) complexes (Table 1). Furthermore, the observed patterns in the ¹H

and ¹³C NMR spectra are in agreement with the proposed symmetric square planar arrangement of the donor atoms around the metal center (i.e., equivalent methyl groups of the SiMe₂ moiety, equivalent tolyl groups, equivalent PPh₂ groups, each containing equivalent phenyl rings).

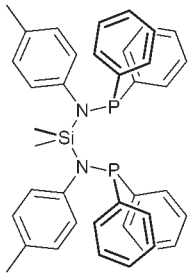
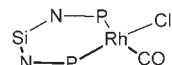
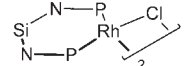
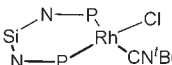
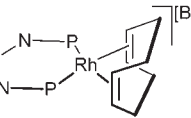
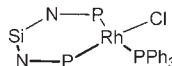
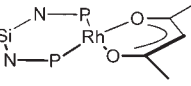
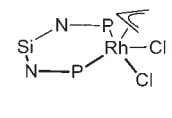
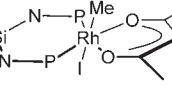
When dealing with the dinuclear structure of **2**, relevant data are in order. The diffusion coefficients of **2** and **4** were measured in C₆D₆ solutions ($D_2 = 4.42 \times 10^{-6}$ cm²/s; $D_4 = 5.88 \times 10^{-6}$ cm²/s), showing that **2** diffuses slower than **4** and as a consequence should be bigger than **4** and as a consequence should be bigger than **4**. Furthermore the ratio D_4/D_2 (1.33) is very close to the calculated value (1.26) for two diffusing species, one (**2**) with a 2-fold volume with respect to the other (**4**).⁷ Also, a sharp lorentzian profile was observed for the ³¹P NMR signal of the mononuclear derivative **4**, whereas the line shape of the ³¹P NMR signal of **2** appeared to be a bit more complex (Figure 1). Definitely, in agreement with the proposed dinuclear structure, the line shape analysis showed that **2** should contain two *magnetically* nonequivalent phosphorus nuclei, and there exist long-range P-to-P (2.0 Hz) and P-to-Rh couplings (–0.4 Hz; Figure 1, cf. Supporting Information).

Finally, it is noteworthy that the structural motif (P₂)Rh(μ-Cl)₂-Rh(P₂) has already been observed in rhodium chemistry (P₂ = two monodentate phosphines or a bidentate one).⁸

The reactions of **2** with CO, CN^tBu, and PPh₃ afford the fragmentation of the dinuclear compounds yielding the corresponding square planar mononuclear rhodium(I) derivative **5**–**7** (Scheme 4).

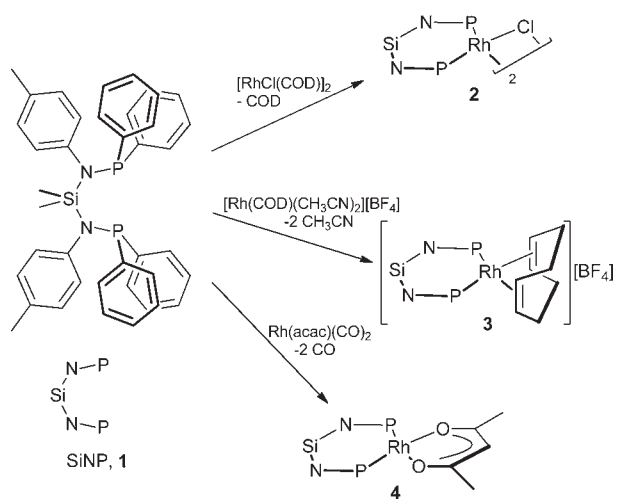
It is worth mentioning that the carbonyl (**5**) and isonitrile (**6**) derivatives are thermally stable and are formed quantitatively upon the reaction of **2** with CO and CN^tBu, respectively. Relevant NMR data are given in Table 1. Similar to **2**–**4**, the ³¹P NMR signals are observed to be downfield shifted with respect to the uncomplexed ligand, and an AX system and a strong dependence of both the chemical shifts and the ¹J_{PRh} coupling constant on the *trans* ligand are observed. Interestingly, the carbonyl stretching IR band of **5** is observed at 2023 cm^{–1}, just between the values observed for PPh₂-based diphosphino⁹ or diphosphinito¹⁰ derivatives of formula RhCl(CO)(P₂), thus indicating an intermediate

Table 1. Selected ^{31}P NMR Data for Compounds 1–10

Compound	δ_{P}	$^1J_{\text{PRh}}$	$^2J_{\text{PP}}$	Compound	δ_{P}	$^1J_{\text{PRh}}$	$^2J_{\text{PP}}$
	49.6 (s)	-	-		75.8 (dd)	168.8	42.1
1				5	67.6 (dd)	132.3	42.1
	86.0 (d ^a)	201.4			80.8 (dd)	184.7	43.3
2				6	76.7 (dd)	139.4	43.3
	66.1 (d)	153.5			78.6 (ddd ^b)	152.3	41.7
3				7	87.6 (ddd ^c)	195.7	41.7
	93.0 (d)	198.7			79.3 (dd)	117.8	21.6
4				8	65.7 (dd)	151.1	21.6
					90.7 (d)	143.9	
				10			

^a $^4J_{\text{PP}} = 2.0$ Hz, $^3J_{\text{PRh}} = -0.4$ Hz (cf. Figure 1 and Supporting Information). ^b $^2J_{\text{PP}}^{\text{trans}} = 365.0$ Hz. ^c $^2J_{\text{PP}}^{\text{cis}} = 33.5$ Hz.

Scheme 3



electron density at the metal center of **5** compared with the mentioned complexes.

The mononuclear $\text{RhCl}(\text{PPh}_3)(\text{SiNP})$ (**7**) derivative was observed in equilibrium with PPh_3 and $[\text{RhCl}(\text{SiNP})]_2$ (**2**; Scheme 4). The thermodynamic parameters of the reaction " $2 + 2 \text{PPh}_3 \rightleftharpoons 2 \text{7}$ " were obtained through variable temperature ^{31}P NMR measurements in the range 303–333 K (cf. Supporting Information). In agreement with the lower $\text{BDE}_{\text{Rh}-\text{Cl}(\text{bridging})}$ vs $\text{BDE}_{\text{Rh}-\text{P}}$,¹¹ the enthalpic variation is negative ($\Delta H_{\text{r}} = -81.5 \pm 0.3$ kJ/mol), and ΔS_{r} is -283 ± 1 ¹² J/molK, reasonably as a consequence of the variation of the overall number of moles ($\Delta n = -1$).

Similar to **5** and **6**, the ^{31}P NMR spectrum of **7** (Table 1) shows downfield shifted signals of the two nonequivalent SiNP phosphorus nuclei which afford an AX system. Furthermore, as expected, the ^{31}P NMR resonance for coordinated PPh_3 is observed as a doublet of doublets of doublets at 32.7 ppm ($^2J_{\text{PP}}^{\text{cis}} = 33.5$, $^2J_{\text{PP}}^{\text{trans}} = 365.0$, $^1J_{\text{PRh}} = 132.6$ Hz).

Finally, no reaction was observed between **2** and weaker π -acceptor ligands such as 1-hexene, styrene, and acrylonitrile, even after prolonged reaction times (up to 72 h) and heating (60 °C), thus reasonably indicating that the stability of the square planar rhodium(I) derivatives of formula $\text{RhCl}(\text{L})(\text{SiNP})$ raises on increasing the π -acceptor ability of L.

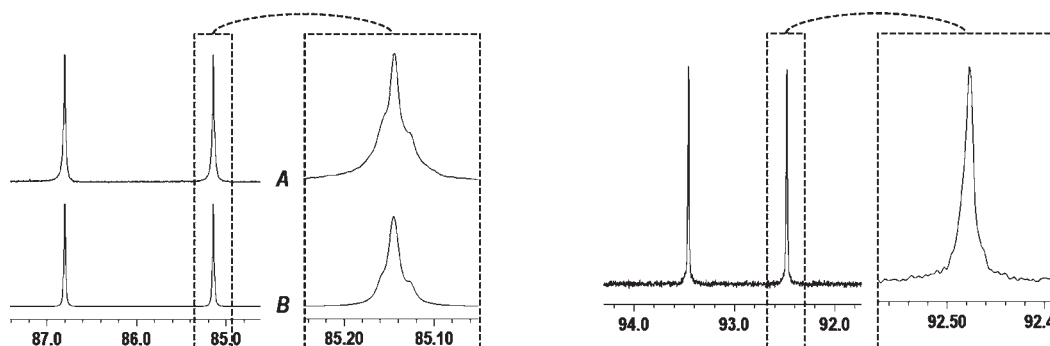
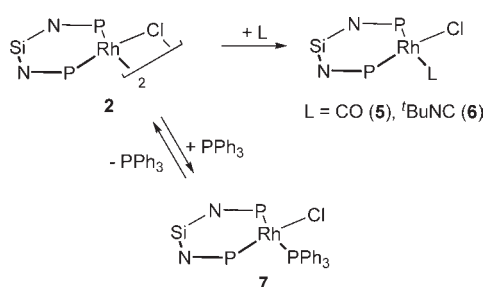
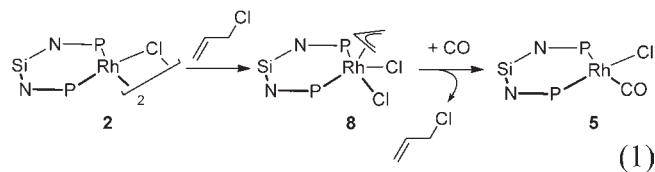


Figure 1. (left) Experimental (A) and simulated (B, $\delta_P = 86.0$ ppm; $^1J_{\text{PRh}} = 201.4$; $^3J_{\text{PRh}} = -0.4$; $^4J_{\text{PP}} = 2.0$ Hz) ^{31}P NMR spectrum of **2** at 298 K (121.45 MHz). (right) ^{31}P NMR (202.47 MHz) spectrum of **4**.

Scheme 4



The oxidative addition of carbon electrophiles such as organic halides is one of the most general routes in order to obtain metal–carbon bonds, which are the key functional groups on the way to the functionalization of organic substrates. Since π -allylic derivatives are well established intermediates in CC bond formation *via* allylation (*vide infra*), the interaction of 3-chloro-1-propene with selected rhodium(I) derivatives among those described above was investigated. The reaction of **2** with 3-chloro-1-propene readily and cleanly affords the oxidative addition product $\text{RhCl}_2(\eta^3\text{-C}_3\text{H}_5)(\text{SiNP})$ (**8**; eq 1). Its solid state structure is shown in Figure 2, along with the coordination polyhedron and a view of the six-membered [PNSiNPRh] ring; selected bond distances and angles are given in Table 2.



A distorted η^3 -coordination [Rh–C(1), 2.138(6) Å; Rh–C(2), 2.204(6) Å; Rh–C(3), 2.331(6) Å; C(1)–C(2), 1.428(9) Å; C(2)–C(3), 1.368(9) Å] of the allyl moiety is observed with rhodium-to-carbon distances (Table 2) similar to those observed in known rhodium(III) allyl complexes.¹³

The coordination sphere of rhodium is completed by two mutually pseudo-*cis* chloride ligands [Rh–Cl(1), 2.466(2) Å; Rh–Cl(2) 2.441(2) Å; Cl(1)–Rh–Cl(2), 90.03(6)°] and by the phosphorus atoms from the chelating SiNP ligand [Rh–P(1), 2.266(2) Å; Rh–P(2), 2.306(2) Å; P(1)–Rh–P(2), 91.35(5)°]. As a consequence, the complex is asymmetric, and indeed two

enantiomers, namely Δ and Λ (Figure 2), are present in the crystal (1:1 ratio; cf. Supporting Information).

As far as the PNSiNP scaffold is concerned, only the platinum complex $\text{PtCl}_2(\text{SiN}^{\text{P}^{\text{y}}\text{P}})^3$ and the azasilatrane derivative $\text{PtCl}_2\text{-}(\text{L})$, L = $\text{EtOSi}(\text{Ph}_2\text{PNCH}_2\text{CH}_2)_2(\text{HNCH}_2\text{CH}_2)\text{N}$,⁴ have been structurally characterized so far (Scheme 1A, B). When comparing¹⁴ $\text{PtCl}_2(\text{SiN}^{\text{P}^{\text{y}}\text{P}})$ and **8**, similar intramolecular distances are observed (Table 2); furthermore, the boat conformations of the six-membered [PNSiNPM] ring of the two complexes are quite similar.

Finally, it is worth mentioning that the observed bite angle (91.35°) and distances (2.266, 2.306 Å) for the coordinated SiNP ligand in **8** are very close to the average values reported by Dierkes and van Leeuwen¹⁵ for the related 1,3-bis-(diphenylphosphino)propane (average bite angle, 91.56°; average M–P distances, 2.29 Å).

The ^{31}P NMR spectrum of **8** shows two nonequivalent phosphorus nuclei as an AX system, indicating that the non-symmetric solid state structure should be preserved in solution (*vide infra*). As far as the allyl moiety is concerned, the expected ^1H and ^{13}C patterns were observed with two nonequivalent methylene and one methyne moiety whose assignment is based on the ^1H – ^1H NOESY, ^1H – ^{13}C HSQC, and ^{13}C NMR spectra, cf. Experimental Section. In this regard, the most relevant observations are the following: the $\text{C}^{\text{a}}\text{H}_2$ methylene protons ($\delta_{\text{H}} = 2.57, 1.64$) show a NOE with the *o*-PPh₂ protons ($\delta_{\text{H}} = 7.99$), while C^{c} is observed as a doublet ($\delta_{\text{C}} = 86.6$, $^2J_{\text{PC}} = 29$ Hz). Thus, as far as the enantiomer Δ is concerned, P¹ should be pseudo-*cis* to C^a and pseudo-*trans* to C^c (Scheme 5B).

When dealing with the SiNP ligand, similar to the solid state structure, both the SiMe₂ methyls and the two SiNP “arms” are nonequivalent (^1H , ^{13}C , cf. Experimental Section), in agreement with the existence of two pairs of nonequivalent semispaces (Scheme 5A) separated by the σ_{v} (left/right) and σ_{h} (up/down) planes, respectively.

Finally, the room temperature ^1H NMR spectrum contains broad aromatic resonances (cf. Experimental Section), so a fluxional process should be going on in solution. Indeed, the ^1H – ^1H EXSY spectrum contains exchange crosspeaks between the methyl signals of the tolyl groups, pointing at the fact that the *left* and *right* semispaces are exchanging. On the other hand, crosspeaks have not been detected between the SiMe₂ methyls, so the *up* and *down* semispaces *do not* exchange (Scheme 5A). On these bases, the fluxionality should rely on the interconversion between the two enantiomers Δ and Λ with the concomitant exchange between P¹ and P² (Scheme 5B).

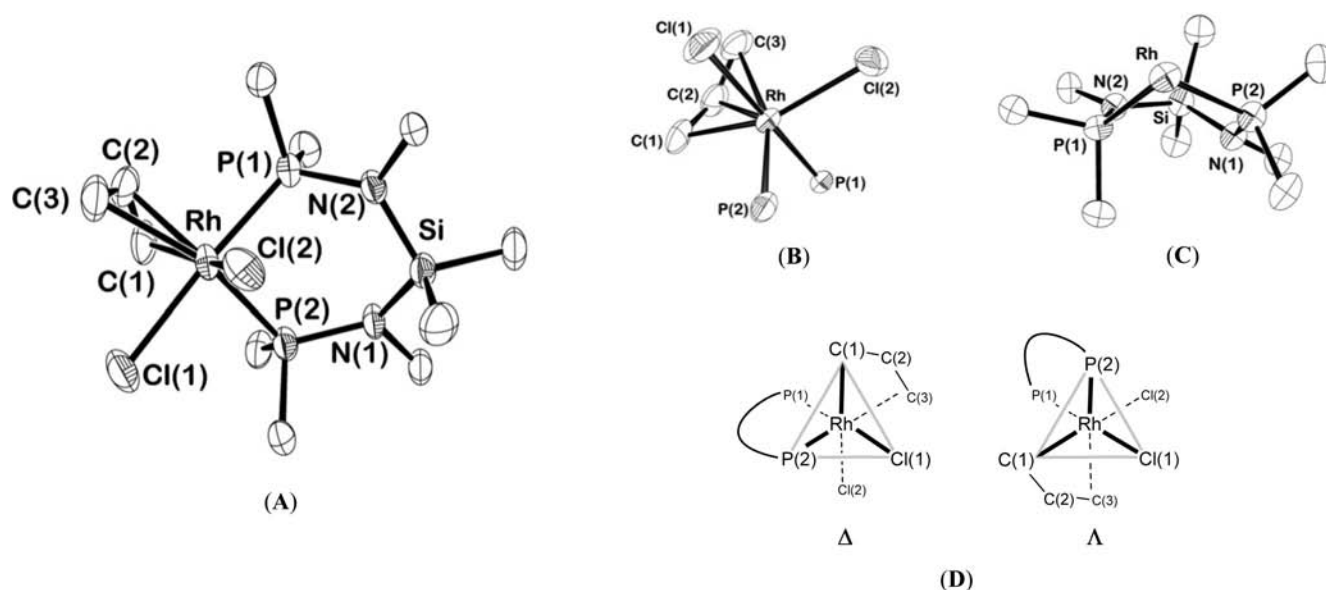
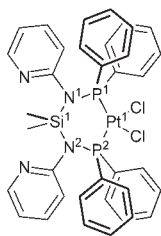


Figure 2. (A) View of the molecular structure of **8** with the numbering scheme adopted (only *ipso* carbons are shown for clarity) with ellipsoids at 50% probability. (B) Coordination polyhedron of **8**. (C) View of the [PNSiNPRh] ring of **8**. (D) Representation of Δ and Λ configurations of **8** as seen in the solid state (cf. Supporting Information).

Table 2. Selected Angles and Bond Distances of **8 and $\text{PtCl}_2(\text{SiN}^{\text{P}^{\text{y}}\text{P}})^3$ with Its Numbering Scheme**

C(1)-C(2)	1.428(9)	Pt(1)-P(2)	2.289(1)
C(2)-C(3)	1.368(9)	Pt(1)-P(1)	2.296(1)
Rh-C(1)	2.138(6)	Si(1)-N(2)	1.785(4)
Rh-C(2)	2.204(6)	Si(1)-N(1)	1.773(4)
Rh-C(3)	2.331(6)	P(1)-N(1)	1.709(4)
Rh-Cl(2)	2.441(2)	P(2)-N(2)	1.713(4)
Rh-Cl(1)	2.466(2)		
Rh-P(1)	2.266(2)		
Rh-P(2)	2.306(2)		
Si-N(2)	1.752(4)		
Si-N(1)	1.761(4)		
P(1)-N(2)	1.677(4)		
P(2)-N(1)	1.701(4)		
P(1)-Rh-P(2)	91.35(5)		
P(1)-Rh-Cl(2)	89.16(5)		
P(2)-Rh-Cl(2)	102.10(6)		
P(1)-Rh-Cl(1)	176.35(5)		
P(2)-Rh-Cl(1)	85.34(6)		
Cl(2)-Rh-Cl(1)	90.03(6)		



At 228 K (in CDCl_3), the exchange slows down, and two nonequivalent PPh_2 moieties are observed also in the ^1H NMR spectrum, each featuring two nonequivalent Ph rings. Also, at 228 K, the rotation of the tolyl rings around the $\text{N}-\text{C}^{\text{ipso}}$ bond is inhibited. The complete assignment of the ^1H , ^{13}C , and ^{31}P NMR signals was carried out using standard 1D and 2D NMR techniques, and reported in the Supporting Information.

The kinetic constants for the $\Delta-\Lambda$ exchange were calculated from ^1H EXSY spectra in the range 283–303 K

(cf. Experimental Section and Supporting Information), and the activation parameters were obtained by the Eyring plot, indicating an intramolecular nondissociative mechanism ($\Delta H_{\text{act}} = 77 \pm 3 \text{ kJ/mol}$, $\Delta S_{\text{act}} = 2 \pm 9^{16} \text{ J/molK}$). Thus, the $\Delta-\Lambda$ interconversion could occur *via* a turn-style mechanism through a trigonal prism intermediate (Scheme 5C).

Finally, as far as **8** is concerned, it should be mentioned that it is indefinitely thermally stable (when stored under an argon atmosphere) but readily reacts with CO (C_6D_6 solution, 1 atm, room temperature), affording 3-chloro-1-propene (^1H , GC-MS) and **5** (^1H , ^{31}P ; eq 1), thus indicating the ability of the [Rh(SiNP)] moiety to promote coupling reactions with the coordinated allyl group.

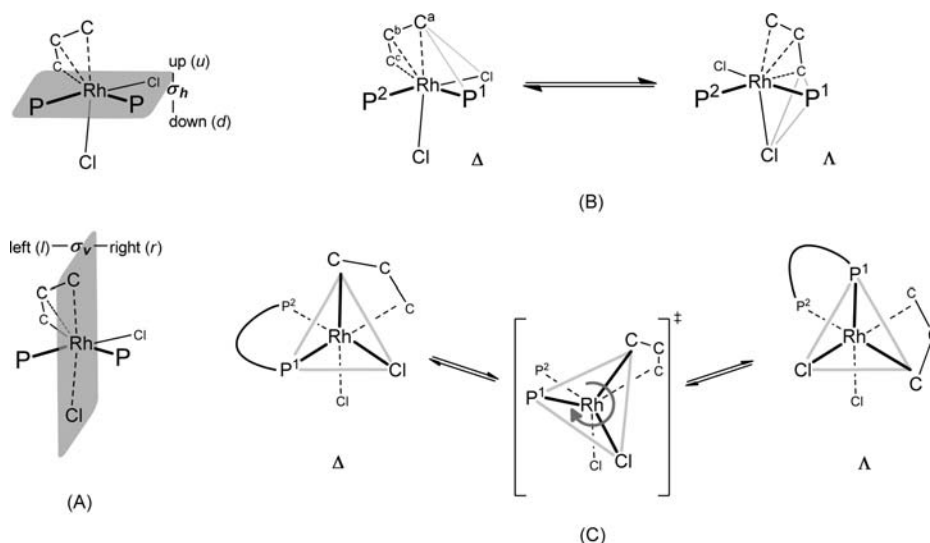
The organic chloride 3-chloro-1-propene also reacts with **4** at room temperature, and the clean formation (3 h) of **2** is observed along with stoichiometric amounts (1:1) of 3-allylpentan-2,4-dione (Scheme 6). In order to clarify the outcome of this reaction, it was carried out at 223 K (acetone- d_6) and two labile intermediates were observed, namely, $\text{Rh}(\eta^1\text{-C}_3\text{H}_5)(\text{Cl})(\text{acac})(\text{SiNP})$ (**9a**) and $[\text{Rh}(\eta^3\text{-C}_3\text{H}_5)(\text{acac})(\text{SiNP})]^+$ (**9b**). Selected NMR data are given in Figure 3.

It is noteworthy that **9b** shows a ^{31}P NMR pattern virtually identical to that of **8** (δ_{P} , $^1J_{\text{PRh}}$ and $^2J_{\text{PP}}$), thus indicating the presence of two nonequivalent phosphorus atoms and suggesting a similar arrangement around the metal center (Figure 3). Furthermore, the ^1H signals of the allyl moiety are indicative of an η^3 -allyl moiety (Figure 3; cf. data for **8**).

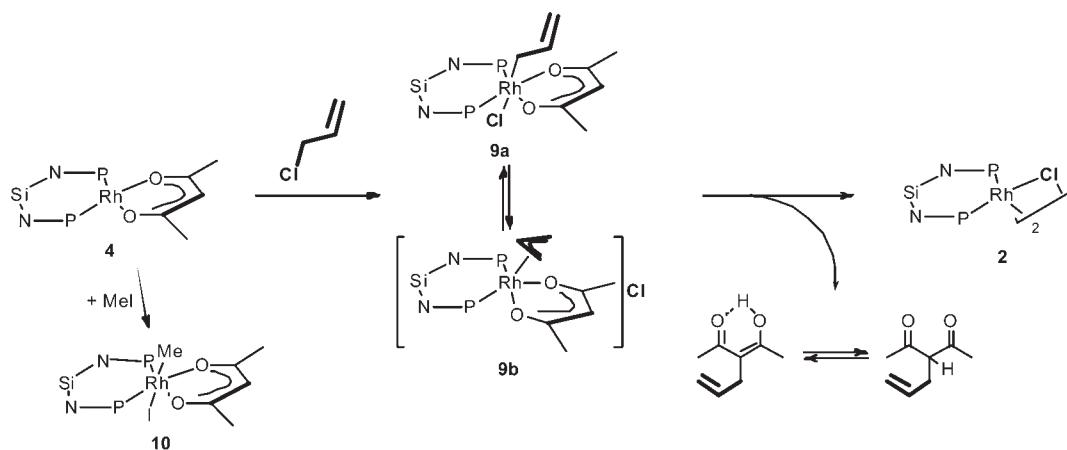
On the other hand, **9a** should contain an η^1 -allyl group and a symmetrically coordinated bidentate SiNP ligand (Figure 3). In this regard, **10** was prepared as a model compound for **9a** by reacting MeI with **4**.¹⁷

Additionally, as far as the equilibrium between **9a** and **9b** is concerned, it is worth mentioning that the $\eta^3-\eta^1$ rearrangement of metallic allylic derivatives has been proposed as the key step responsible for the loss of regioselectivity in allylic alkylation reactions.¹⁸

Scheme 5



Scheme 6



CONCLUSIONS

The novel ligand $\text{SiMe}_2(\text{NtolPPH}_2)_2$ (SiNP) featuring a PNSiNP scaffold could be prepared by a step-by-step synthesis based on the aminolysis of the P–Cl bond of PClPh_2 and the following Cl/amido metathesis in SiMe_2Cl_2 . The presence of nitrogen and phosphorus atoms suggests that the SiNP molecule could act as either a $\kappa^2\text{-N,N}'$, $\kappa^2\text{-P,P}'$, or $\kappa\text{-N}/\kappa\text{-P}$ ligand. Nevertheless, the reactivity of SiNP toward rhodium(I) indicates that diphosphine-like coordination is preferred; indeed, complexes **2–7** exhibit a $\kappa^2\text{-P,P}'$ coordinated SiNP ligand. When compared with the structurally related 1,3-bis(diphenylphosphino)propane, SiNP features similar bite angles and distances. Nevertheless, the overall structure appears to be more hindered, probably due to the congestion within methyl, N-tolyl, and P-phenyl substituents. Definitely, low temperature NMR measurements of selected compounds showed the hindered rotation of these rings. On the other hand, the presence of the nitrogen atom attached to the phosphorus atom reduces the basicity of this atom, as confirmed by the frequency of the stretching band of the CO ligand of **5**.

As far as the reactivity of the above-mentioned rhodium(I) complexes is concerned, this study indicates that selected rhodium(I) species can be cleanly oxidized by organic halides, namely, methyl iodide and allyl chloride. In the resulting compounds **8–10**, the coordination of the SiNP ligand is retained, and no side-reactions have been detected (e.g., electrophilic attack to the uncoordinated nitrogen atoms). Furthermore, the stability/behavior of the oxidized organometallic species is observed to depend on the ancillary ligands. The chloride allyl derivative **8** is chiral (Δ , Λ), and the enantiomers interconvert by an intramolecular pathway through of a prism-like activation state (Scheme 5). On the other hand, the η^3 -allyl cation **9b**, isoelectronic with **8**, could be observed only at low temperatures in equilibrium with the related η^1 -allyl complex **9b**. To the best of our knowledge, this η^1 – η^3 equilibrium has been claimed in order to justify the loss of regioselectivity in rhodium-catalyzed allylation reactions but never directly observed.¹⁸

EXPERIMENTAL SECTION

All of the operations were carried out using standard Schlenk-tube techniques under an atmosphere of prepurified argon or in a Braun

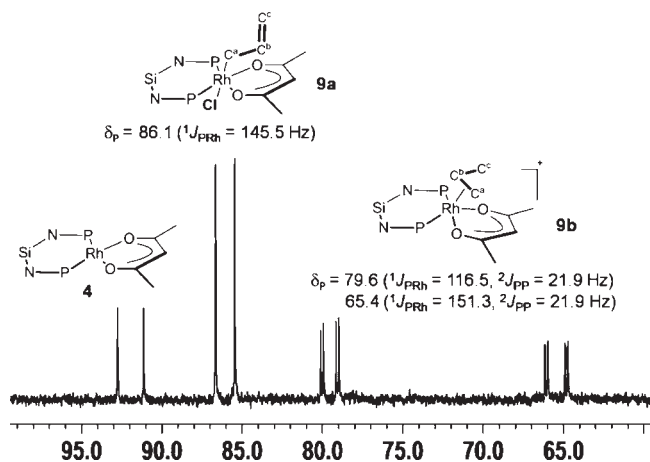


Figure 3. ^{31}P NMR spectrum (acetone- d_6 , 233 K) of the reaction mixture obtained after adding 3-chloro-1-propene to $\text{Rh}(\text{acac})(\text{SiNP})$ (4), with the proposed assignment. Selected ^1H NMR data are in order: 9a, $\delta_{\text{H}} = 1.13$ ($\text{C}^{\text{a}}\text{H}_2$), 5.24 ($\text{C}^{\text{b}}\text{H}$), 4.21 and 4.30 ($\text{C}^{\text{c}}\text{H}_2$), 5.23 (CH^{acac}). 9b, $\delta_{\text{H}} = 1.49$ and 2.40 ($\text{C}^{\text{a}}\text{H}_2$), 5.10 ($\text{C}^{\text{b}}\text{H}$), 4.35 and 4.82 ($\text{C}^{\text{c}}\text{H}_2$), 5.41 (CH^{acac}).

glovebox under dinitrogen. The solvents were dried and purified according to standard procedures. NH_2tol (Aldrich), PClPh_2 (Aldrich), SiMe_2Cl_2 (Aldrich), $\text{CH}_2\text{CHCH}_2\text{Cl}$ (Aldrich), PPh_3 (Aldrich), CN^tBu (Aldrich), and CO (Praxair) were commercially available and were used as received if not otherwise stated.

NMR spectra were measured with Bruker spectrometers (AV300, AV400, AV500) and are referred to SiMe_4 (^1H , ^{13}C) and H_3PO_4 (^{31}P). Infrared spectra were recorded on a Thermo Nicolet Avatar 360 FT-IR spectrometer. Elemental analyses were performed by using a Perkin–Elmer 2400 microanalyzer. Mass spectra (MALDI) were recorded with a Bruker MicroFlex spectrometer using DCTB (1,1-dicyano-4-*t*-butylphenyl-3-methylbutadiene) as a matrix.

The diffusion experiments were performed using the stimulated echo pulse sequence¹⁹ without spinning. The shape of the gradient pulse was rectangular, and its strength varied automatically in the course of the experiments. The diffusion coefficients (D) were determined from the slope of the regression line $\ln(I/I_0)$ versus G^2 according to $\ln(I/I_0) = -(\gamma\delta)^2(\Delta - \delta/3)DG^2$, in which I and I_0 are the observed spin echo intensity with and without gradients, respectively, G is the gradient strength, Δ is the delay between the midpoints of the gradients, D is the diffusion coefficient, and δ is the gradient length. The calibration of the gradients was carried out by a diffusion measurement of HDO in D_2O . The experimental error in the D values was estimated to be 2%. All of the data leading to the reported D values afforded lines with correlation coefficients of >0.999 , and 10–16 points were used for regression analysis. The value for the δ parameter was set to 1.75–2 ms. Additionally, three different measurements with different diffusion parameters ($\Delta = 25$ –100 ms) were always carried out to check the reproducibility of the data obtained. The gradient strength was increased in 5–8% steps. A measurement of the ^1H NMR spectrum and T_1 was carried out before each diffusion experiment and the recovery delay (approx. 5–8 s) set to 5 times T_1 . The number of scans varied between 32 and 64 per increment. The typical experiment duration was 1.5–3 h.

Synthesis of $\text{SiMe}_2[\text{N}(\text{tol})\text{PPh}_2]_2$ (1, SiNP). *a. Synthesis of $\text{NH}(\text{tol})\text{PPh}_2$.* Freshly sublimed NH_2tol (3.38 g, 31.5 mmol) was treated with PClPh_2 (2.80 mL, $d = 1.194$ g/mL, 15.2 mmol) in THF (100 mL). The ready precipitation of a colorless solid was observed. After 30 min of stirring, the solid was filtered off and the filtrate evaporated, thus yielding a colorless solid identified as $\text{NH}(\text{tol})\text{PPh}_2$ (3.40 g, 77% yield). Found: C, 78.51; H, 6.45; N, 4.75. Calcd for $\text{C}_{19}\text{H}_{18}\text{NP}$ (291.33): C, 78.33; H,

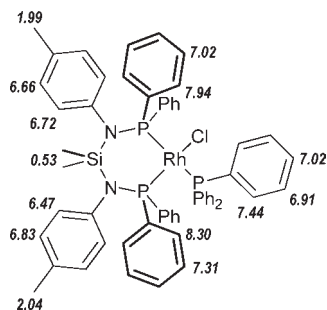
6.23; N, 4.81. ^1H NMR (CDCl_3 , 298 K): δ 7.52 (m, 4H, *o*-PPh), 7.45–7.40 (6H, *m*-PPh + *p*-PPh), 7.04 (d, 2H, $^3J_{\text{HH}} = 8.0$ Hz, $\text{C}^3\text{H}^{\text{tol}}$), 6.83 (d, 2H, $^3J_{\text{HH}} = 8.0$ Hz, $\text{C}^2\text{H}^{\text{tol}}$), 4.37 (br, 1H, NH), 2.29 (s, 3H, CH_3^{tol}). ^{13}C NMR (CDCl_3 , 298 K): δ 144.1 (d, $^1J_{\text{CP}} = 17$ Hz, *ipso*-PPh), 140.4 (d, $^2J_{\text{CP}} = 12$ Hz, $\text{C}^{1\text{-tol}}$), 131.2 (d, $^2J_{\text{CP}} = 20$ Hz, *o*-PPh), 129.82 (s, $\text{C}^{3\text{-tol}}$), 129.03 (s, *p*-PPh), 128.79 (s, $\text{CCH}_3^{\text{tol}}$), 128.59 (d, $^3J_{\text{CP}} = 5$ Hz, *m*-PPh), 116.1 (d, $^3J_{\text{CP}} = 12$ Hz, $\text{C}^{2\text{-tol}}$), 20.5 (s, CH_3^{tol}). ^{31}P NMR (CDCl_3 , 298 K): δ , 28.7 (s).

b. Reaction of $\text{NH}(\text{tol})\text{PPh}_2$ with BuLi and SiMe_2Cl_2 . A solution of $\text{NH}(\text{tol})\text{PPh}_2$ (1.74 g, 5.97 mmol) in THF (8 mL) + toluene (20 mL) at 198 K was treated with $^n\text{BuLi}$ (1.6 M in hexane, 3.70 mL, 5.92 mmol). The mixture was allowed to warm up to room temperature (2 h), and SiMe_2Cl_2 (0.360 mL, 2.98 mmol, $d = 1.07$ g/mL) was added. After stirring overnight at room temperature, the suspension was heated at 333 K for 3 h. All of the volatiles were removed *in vacuo*, and the residue was extracted with CH_2Cl_2 . The liquid phase was concentrated and hexane added, thus affording the precipitation of a colorless solid, which was filtered off, washed with Et_2O , dried *in vacuo*, and finally identified as $\text{SiMe}_2[\text{N}(\text{tol})\text{PPh}_2]_2$ (1, SiNP, 1.30 g, 68% yield). Found: C, 75.25; H, 6.18; N, 4.42. Calcd for $\text{C}_{40}\text{H}_{40}\text{N}_2\text{P}_2\text{Si}$ (638.79): C, 75.20; H, 6.31; N, 4.39. ^1H NMR (CDCl_3 , 298 K): δ 7.35–7.23 (10H, PPh), 6.79 (d, 2H, $^3J_{\text{HH}} = 8.2$ Hz, $\text{C}^3\text{H}^{\text{tol}}$), 6.54 (d, 2H, $^3J_{\text{HH}} = 8.2$ Hz, $\text{C}^2\text{H}^{\text{tol}}$), 2.26 (s, 3H, CH_3^{tol}), 0.54 (s, 3H, SiCH_3). ^{13}C NMR (CDCl_3 , 298 K): δ 141.6 (m, *ipso*-PPh), 139.4 (m, $\text{C}^{1\text{-tol}}$), 134.1 (s, $\text{C}^{4\text{-tol}}$), 133.6 (m, *o*-PPh), 130.4 (s, $\text{C}^{2\text{-tol}}$), 128.6 (s, $\text{C}^{3\text{-tol}}$), 128.4 (s, *p*-PPh), 127.6 (m, *m*-PPh), 20.9 (s, CH_3^{tol}), 2.3 (t, $^3J_{\text{CP}} = 9.6$ Hz, SiCH_3). ^{31}P NMR (CDCl_3 , 298 K): δ , 49.6 (s).

Synthesis of $[\text{RhCl}(\text{SiNP})]_2$ (2). A yellow solution of $[\text{RhCl}(\text{COD})]_2$ (80.8 mg, 0.164 mmol) in CH_2Cl_2 (5 mL) was treated with SiNP (209 mg, 0.327 mmol). The solution readily changed to red-orange. After 30 min of stirring, the solution was concentrated and Et_2O (5 mL) added, thus yielding the precipitation of a deep orange solid, which was filtered off, washed with Et_2O (2 mL), dried *in vacuo*, and finally identified as $[\text{RhCl}(\text{SiNP})]_2$ (2, 194 mg, 76% yield). Found: C, 62.00; H, 5.21; N, 3.45. Calcd for $\text{C}_{40}\text{H}_{40}\text{ClN}_2\text{P}_2\text{RhSi}$ (777.15): C, 61.82; H, 5.19; N, 3.60. ^1H NMR (C_6D_6 , 298 K): δ 7.69 (m, 4H, *o*-PPh), 7.04 (t, $^3J_{\text{HH}} = 7.2$ Hz, 2H, *p*-PPh), 6.92 (t, $^3J_{\text{HH}} = 7.3$ Hz, 4H, *m*-PPh), 6.72 (d, $^3J_{\text{HH}} = 8.2$ Hz, 2H, $\text{C}^2\text{H}^{\text{tol}}$), 6.56 (d, $^3J_{\text{HH}} = 8.2$ Hz, 2H, $\text{C}^3\text{H}^{\text{tol}}$), 1.88 (s, 3H, CH_3^{tol}), 0.73 (s, 3H, SiCH_3). ^{13}C NMR (C_6D_6 , 298 K): δ 141.8 (m, $\text{C}^{1\text{-tol}}$), 137.5 (m, *ipso*-PPh), 134.9 (m, *o*-PPh), 134.5 (s, $\text{C}^{4\text{-tol}}$), 131.1 (s, $\text{C}^{2\text{-tol}}$), 129.0 (s, $\text{C}^{3\text{-tol}}$), 128.5 (s, *p*-PPh), 126.7 (m, *m*-PPh), 20.7 (s, CH_3^{tol}), 4.1 (t, $^3J_{\text{CP}} = 2.95$, SiCH_3). ^{31}P NMR: 86.0 (m, $^1J_{\text{PRh}} = 201.4$ Hz, $^4J_{\text{PP}} = 2.0$ Hz, $^3J_{\text{PRh}} = -0.4$ Hz), cf. Results and Discussion, and Supporting Information for further details. MS (MALDI⁺, DCTB): m/z 1552.2 (M^+ , 2%), 791.1 ($[\text{M}/2 + \text{CH}_3]^+$, 15%), 775.1 ($[\text{M}/2 - \text{H}]^+$, 50%), 761.2 ($[\text{M}/2 - \text{CH}_3]^+$, 55%), 757.2 ($[\text{M}/2 - \text{CH}_3 - 4\text{H}]^+$, 100%).

Synthesis of $[\text{Rh}(\text{SiNP})(\text{COD})][\text{BF}_4]$ (3). A solution of $[\text{Rh}(\text{COD})(\text{CH}_3\text{CN})_2][\text{BF}_4]$ (129 mg, 0.339 mmol) in CH_2Cl_2 (10 mL) was treated with SiNP (220 mg, 0.344 mmol). After 30 min of stirring, the solution was concentrated and hexane added, thus yielding the precipitation of a yellow solid, which was filtered off, dried *in vacuo*, and finally identified as $[\text{Rh}(\text{COD})(\text{SiNP})][\text{BF}_4]$ (3, 251 mg, 79% yield). Found: C, 61.89; H, 5.48; N, 2.85. Calcd for $\text{C}_{48}\text{H}_{52}\text{BF}_4\text{N}_2\text{P}_2\text{RhSi}$ (936.68): C, 61.55; H, 5.60; N, 2.99. ^1H NMR (CD_2Cl_2 , 298 K): δ 7.50–7.40 (12H, *o*-PPh + *p*-PPh), 7.33 (t, $^3J_{\text{HH}} = 7.3$ Hz, 8H, *m*-PPh), 6.84 (d, $^3J_{\text{HH}} = 8.1$ Hz, 4H, $\text{C}^3\text{H}^{\text{tol}}$), 6.66 (d, $^3J_{\text{HH}} = 8.1$ Hz, 4H, $\text{C}^2\text{H}^{\text{tol}}$), 4.66 (br, 4H, CH^{COD}), 2.40–2.24 (8H, CH_2^{COD}), 2.19 (s, 6H, CH_3^{tol}), 0.74 (s, 6H, SiCH_3). ^{13}C NMR (CD_2Cl_2 , 298 K): δ 139.3 (m, $\text{C}^{1\text{-tol}}$), 136.4 (s, $\text{C}^{4\text{-tol}}$), 133.5 (m, *o*-PPh), 131.3 (s, *p*-PPh), 130.8 (m, *ipso*-PPh), 129.4 ($\text{C}^{2\text{-tol}} + \text{C}^{3\text{-tol}}$), 128.8 (m, *m*-PPh), 100.4 (dt, $J = 7.3, 4.9$; CH^{COD}), 30.5 (s, CH_2^{COD}), 20.46 (s, CH_3^{tol}), 3.29 (t, $^3J_{\text{CP}} = 3.8$, SiCH_3). ^{31}P NMR (CD_2Cl_2 , 298 K): δ 66.1 (d, $^1J_{\text{PRh}} = 153.5$ Hz). MS (MALDI⁺, DCTB): m/z 849.2 (M^+ , 17%), 741.1 ($[\text{M} - \text{COD}]^+$, 100%).

Scheme 7

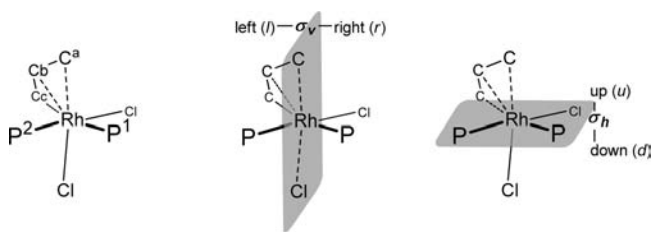


Synthesis of Rh(acac)(SiNP) (4). A toluene (10 mL) solution of Rh(acac)(CO)₂ (145 mg, 0.562 mmol) was treated with SiNP (360 mg, 0.564 mmol). The prompt evolution of gas was observed along with a color change from yellow-green to orange. After 30 min of stirring, the solution was concentrated and hexane added (20 mL), thus yielding the precipitation of an orange solid, which was filtered off, dried *in vacuo*, and identified as Rh(acac)(SiNP) (4, 308 mg, 65% yield). Found: C, 64.01; H, 5.55; N, 3.48. Calcd for C₄₅H₄₇N₂O₂P₂RhSi (840.81): C, 64.28; H, 5.63; N, 3.33. ¹H NMR (C₆D₆, 298 K): δ 8.03 (m, 8H, *o*-PPh), 7.23 (t, ³J_{HH} = 7.2 Hz, 4H, *p*-PPh), 7.18 (t, ³J_{HH} = 7.3 Hz, 8H, *m*-PPh), 6.93 (d, ³J_{HH} = 8.2 Hz, 4H, C²H^{tol}), 6.74 (d, ³J_{HH} = 8.2 Hz, 4H, C³H^{tol}), 5.30 (s, 1H, CH^{acac}), 2.03 (s, 6H, CH₃^{tol}), 1.63 (s, 6H, CH₃^{acac}), 0.98 (s, 6H, SiCH₃). ¹³C NMR (C₆D₆, 298 K): δ 184.2 (s, CO), 141.5 (m, C^{1-tol}), 137.2 (m, *ipso*-PPh), 134.7 (m, *o*-PPh), 134.6 (s, C^{4-tol}), 131.1 (s, C^{2-tol}), 129.0 (s, C^{3-tol}), 128.6 (s, *p*-PPh), 126.7 (m, *m*-PPh), 99.7 (d, J = 1.9 Hz, CH^{acac}), 26.9 (td, J = 3.5, 0.8, CH₃^{acac}), 20.6 (s, CH₃^{tol}), 3.86 (t, ³J_{CP} = 3.1, SiCH₃). ³¹P NMR (C₆D₆, 298 K): δ 93.0 (d, ¹J_{PRh} = 198.7 Hz).

Reaction of [RhCl(SiNP)]₂ with PPh₃, CO, CN^tBu. *a.* CO. A toluene solution (5 mL) of [RhCl(SiNP)]₂ (2, 150 mg, 96.5 μmol) was bubbled with CO over 10 min, thus turning deep yellow. On standing (approximately 1 h), the precipitation of a yellow solid was observed; it was filtered off, dried *in vacuo*, and identified as RhCl(SiNP)(CO) (5, 116 mg, 75% yield). Found: C, 61.25; H, 4.95; N, 3.47. Calcd for C₄₁H₄₀ClN₂OP₂RhSi (805.16): C, 61.16; H, 5.01; N, 3.48. ¹H NMR (acetone-*d*₆, 298 K): δ 7.65 (m, 4H, *o*-P¹Ph), 7.55 (m, 4H, *o*-P²Ph), 7.44 (t, ²J_{HH} = 7.4, 4H, *p*-P¹Ph + *p*-P²Ph), 7.30 (t, ³J_{HH} = 7.6, 8H, *m*-P¹Ph + *m*-P²Ph), 6.87 (d, ³J_{HH} = 8.2, 2H, C³H^{tol2}), 6.80 (d, ³J_{HH} = 8.2, 2H, C³H^{tol1}), 6.73 (d, ³J_{HH} = 8.2, 2H, C²H^{tol2}), 6.57 (d, ³J_{HH} = 8.2, 2H, C²H^{tol1}), 2.18 (s, 3H, CH₃^{tol2}), 2.14 (s, 3H, CH₃^{tol1}), 0.48 (s, 6H, SiCH₃). ¹³C NMR (acetone-*d*₆, 298 K): δ 187.7 (ddd, J = 14.6, 65.6, 122.2 Hz, CO), 140.1 (d, ²J_{CP} = 9.8, C^{1-tol2}), 139.8 (d, ²J_{CP} = 9.8, C^{1-tol1}), 137.1 (d, ¹J_{CP} = 56.9, *ipso*-PPh), 135.8 (s, C^{4-tol2}), 135.5 (s, C^{4-tol1}), 134.8 (d, ²J_{CP} = 11.9, *o*-P¹Ph), 133.5 (d, ²J_{CP} = 12.4, *o*-P²Ph), 132.6 (d, ¹J_{CP} = 48.7, *ipso*-PPh), 130.8 (s, C^{2-tol2}), 130.6 (s, C^{2-tol1}), 130.2 (d, ⁴J_{CP} = 2.0, *p*-P²Ph), 130.0 (d, ⁴J_{CP} = 2.0, *p*-P¹Ph), 129.1 (s, C^{3-tol2}), 128.9 (s, C^{3-tol1}), 127.5 (d, ³J_{CP} = 10.6, *m*-P¹Ph), 127.2 (d, ³J_{CP} = 10.6, *m*-P²Ph), 19.94 (s, CH₃^{tol2}), 19.87 (s, CH₃^{tol1}), 2.63 (t, ³J_{CP} = 3.3, SiCH₃). ³¹P NMR (acetone-*d*₆, 298 K): δ 75.8 (dd, ²J_{PP} = 42.1, ¹J_{PRh} = 168.8, P²), 67.6 (dd, ²J_{PP} = 42.1; ¹J_{PRh} = 132.3, P¹). IR (CH₂Cl₂): 2023 cm⁻¹ (ν_{CO}).

b. CN^tBu. A toluene solution (10 mL) of [RhCl(SiNP)]₂ (2, 160 mg, 0.103 mmol) was treated with CN^tBu (23.3 μL, *d* = 0.735 g/mL, 0.206 mmol). The solution readily turned pale yellow. After 30 min of stirring, the volatiles were removed *in vacuo* and the residue recrystallized from toluene/hexane and identified as RhCl(SiNP)(CN^tBu) (6, 152 mg, 86% yield). Found: C, 63.10; H, 5.70; N, 4.91. Calcd for C₄₅H₄₉ClN₃-P₂RhSi (860.28): C, 62.83; H, 5.74; N, 4.88. ¹H NMR (C₆D₆, 298 K): δ 8.20 (m, 4H, *o*-P²Ph), 7.96 (m, 4H, *o*-P¹Ph), 7.21–7.11 (12H, *m*-P¹Ph + *m*-P²Ph + *p*-P¹Ph + *p*-P²Ph), 6.86 (d, ³J_{HH} = 7.7 Hz, 2H, C²H^{tol2}), 6.76 (d, ³J_{HH} = 8.2 Hz, 2H, C²H^{tol1}), 6.74 (d, ³J_{HH} = 7.7 Hz, 2H, C³H^{tol2}),

Scheme 8



6.67 (d, ³J_{HH} = 8.20 Hz, 2H, C³H^{tol1}), 2.04 (s, 3H, CH₃^{tol2}), 1.99 (s, 3H, CH₃^{tol1}), 0.76 (s, 9H, CH₃^{tBu}), 0.69 (s, 6H, SiCH₃). ¹³C NMR (C₆D₆, 298 K): δ 141.9 (dd, ²J_{CP} = 11.0, ⁴J_{CP} = 2.1, C^{1-tol2}), 141.4 (dd, ²J_{PP} = 10.1, ⁴J_{PP} = 1.7, C^{1-tol1}), 139.6 (d, ¹J_{CP} = 51.4, *ipso*-P¹Ph), 135.33 (d, ¹J_{CP} = 46.7, *ipso*-P²Ph), 135.30 (d, ²J_{CP} = 11.9, *o*-P²Ph), 134.95 (d, ⁵J_{CP} = 1.5, C^{4-tol2}), 134.67 (d, ⁵J_{CP} = 1.4, C^{4-tol1}), 134.45 (d, ²J_{CP} = 12.5, *o*-P¹Ph), 131.1 (d, ⁴J_{CP} = 1.9, C^{3-tol2}), 130.9 (d, ⁴J_{CP} = 1.8, C^{3-tol1}), 129.1 (s, C^{2-tol2}), 129.0 (d, ³J_{CP} = 1.7, *p*-P²Ph), 128.9 (C^{2-tol1} + *p*-P¹Ph), 127.0 (d, ³J_{CP} = 10.0, *m*-PPh), 55.5 (br, C^{tBu}), 29.4 (s, CH₃^{tBu}), 20.58 (s, CH₃^{tol2}), 20.50 (s, CH₃^{tol1}), 3.8 (s, SiCH₃). ³¹P NMR (C₆D₆, 298 K): δ 80.8 (dd, ¹J_{PRh} = 184.7, ²J_{PP}^{cis} = 43.3, P¹), 76.7 (dd, ¹J_{PRh} = 139.4, ²J_{PP}^{cis} = 43.3, P²).

c. PPh₃. In a NMR tube, [RhCl(SiNP)]₂ (2, 15.3 mg, 9.84 μmol) was dissolved in C₆D₆ (0.379 g, *d* = 0.950 g/mL, 0.399 mL). Sequentially, PPh₃ (5.8 mg, 22 μmol) was added, thus affording an orange solution. The mixture was analyzed by ¹H and ³¹P NMR spectroscopy, proving to be an equilibrium mixture of [RhCl(SiNP)]₂ (δ_P = 86.1, d, ¹J_{PRh} = 201.8 Hz), PPh₃ (δ_P = -5.1, s) and RhCl(SiNP)(PPh₃) (7; *vide infra*). The determination of the thermodynamic parameters of the equilibrium (ΔH_r = -81.5 ± 0.3 kJ/mol; ΔS_r = -282 ± 1 J/molK) was carried out through variable temperature ³¹P NMR measurements in the range 303–333 K (cf. Supporting Information). Selected NMR data of RhCl(SiNP)(PPh₃) (7) are in order. ³¹P NMR (C₆D₆, 293 K): δ 32.7 (ddd, ²J_{PP}^{trans} = 365.0, ¹J_{PRh} = 132.6, ²J_{PP}^{cis} = 33.5, 1P, PPh₃), 78.6 (ddd, ²J_{PP}^{trans} = 365.0, ¹J_{PRh} = 152.3, ²J_{PP}^{cis} = 41.7, 1P, P *trans* to PPh₃), 87.6 (ddd, ¹J_{PRh} = 195.7, ²J_{PP}^{cis} = 41.7, 33.5, 1P, P *cis* to PPh₃). Scheme 7 shows the assigned δ_H of 7 based on ¹H–¹H COSY, ¹H–¹H NOESY, and ¹H–³¹P HMBC spectra.

Synthesis of RhCl₂(η³-C₃H₅)(SiNP) (8). A toluene solution (15 mL) of [RhCl(SiNP)]₂ (2, 242 mg, 0.156 mmol) was treated with 3-chloro-1-propene (25.5 μL, 0.939 g/mL, 0.313 mmol). The solution was allowed to stand overnight, yielding the abundant precipitation of a pale yellow microcrystalline solid which was filtered off, washed with Et₂O (2 × 3 mL), dried *in vacuo*, and identified as RhCl₂(η³-C₃H₅)(SiNP) (8, 189 mg, 71% yield). Found: C, 61.01; H, 5.42; N, 3.15. Calcd for C₄₃H₄₅Cl₂N₂P₂RhSi (853.67): C, 60.50; H, 5.31; N, 3.28. ¹H NMR (CD₂Cl₂, 298 K, δ_C as obtained from ¹H ¹³C HSQC spectrum, cf. Scheme 8 for labeling): δ 9.07 (very br, no integrable), 7.99 (m, 2H, PPh, δ_C = 132.8), 7.94 (t, ²J_{HH} = 7.5, 1H, PPh, δ_C = 131.5), 7.86 (m, 2H, PPh, δ_C = 128.9), 7.53 (t, ²J_{HH} = 7.6, 1H, PPh, δ_C = 130.5), 7.43 (d, ²J_{HH} = 7.9, 1H, C²H^t, δ_C = 133.8), 7.31 (b, 2H, PPh, δ_C = 126.3), 7.22 (t, ²J_{HH} = 6.7, 1H, PPh, δ_C = 131.1), 7.18 (d, ²J_{HH} = 7.9, 2H, C²H^t + C²H^r, δ_C = 129.1, 131.8), 7.12 (br, 2H, PPh, δ_C = 131.1), 7.04 (d, ²J_{HH} = 8.5, 1H, C³H^t, δ_C = 128.9), 7.00 (m, 2H, PPh, δ_C = 126.8), 6.80 (d, ²J_{HH} = 8.50, 1H, C³H^r, δ_C = 129.1), 6.67–6.61 (3H, PPh + C³H^t + C³H^r, δ_C = 130.4, 128.4), 5.47 (d, ²J_{HH} = 8.2, 1H, C²H^{r/t}, δ_C = 131.8), 5.09 (m, 1H, C²H, δ_C = 109.5), 5.02 (dd, J = 8.3, 13.7, 1H, C²H^{trans}, δ_C = 86.6, ²J_{CP} = 29 Hz), 4.63 (t, J = 7.1, C²H^{cis}, δ_C = 86.6, ²J_{CP} = 29 Hz), 2.57 (d, J = 11.3, 1H, C³H^{trans}, δ_C = 55.7), 2.22 (s, 3H, CH₃^{tol1}, δ_C = 20.4), 2.08 (d, J = 2.08, 3H, CH₃^{tolr}, δ_C = 20.3), 1.64 (dq, J = 6.6, 2.0, C³H^{cis}, δ_C = 55.7), 0.89 (s, 3H, SiCH₃^d, δ_C = 2.19), -0.27 (s, 3H, SiCH₃^u, δ_C = 2.29). ³¹P NMR (CD₂Cl₂, 298 K, cf. Scheme 8 for labeling): δ 79.3 (dd, ¹J_{PRh} = 117.8, ²J_{PP}^{cis} = 21.6, P²), 65.7 (dd, ¹J_{PRh} = 151.1, ²J_{PP}^{cis} = 21.6, P¹).

Table 3. Crystal Data and Structure Refinement Parameters for $\text{RhCl}_2(\eta^3\text{-C}_3\text{H}_5)(\text{SiNP}) \cdot 2\text{CH}_2\text{Cl}_2$ ($8 \cdot 2\text{CH}_2\text{Cl}_2$)

formula	$\text{C}_{45}\text{H}_{49}\text{Cl}_6\text{N}_2\text{P}_2\text{RhSi}$
fw	1023.50
cryst syst	triclinic
space group	$P\bar{1}$
a , Å	9.778(2)
b , Å	10.863(2)
c , Å	22.465(3)
α , deg	87.49(3)
β , deg	87.66(3)
γ , deg	88.64(3)
V , Å ³	2381.3(7)
Z	2
D_{calcd} , g cm ⁻³	1.427
T , K	293(2)
$\mu(\text{Mo K}\alpha)$, mm ⁻¹	0.821
no. reflns measd	8843
no. obsd reflns [$I \geq 2\sigma(I)$]	7403
$R = \sum F_o - F_c / \sum F_o $	0.064
$R_w = \{\sum [w(F_o^2 - F_c^2)^2] / \sum [w(F_o^2)^2]\}^{1/2}$	0.146
GO F	1.252

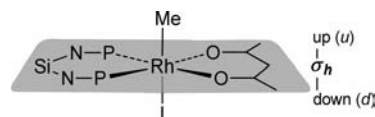
The fluxional behavior of **8** was investigated via $^1\text{H}-^1\text{H}$ EXSY and the activation parameters obtained from the Eyring plot over the temperature range 283–303 K (cf. Supporting Information; $\Delta H_{\text{act}} = 77 \pm 3$ kJ/mol; $\Delta S_{\text{act}} = 2 \pm 9$ J/mol K). The crosspeaks between signals of the two nonequivalent tolyl C^4 Me groups were used to calculate the exchange rate constants (k) given in the Supporting Information; $k = I_K / [t_M(I_K + I_D)]$, where I_D and I_K are the diagonal and crosspeak integrals, respectively, and t_M = mixing time (1.0 s).

^{31}P NMR (CDCl_3 , 228 K): δ 79.5 (dd, $^1J_{\text{PRh}} = 118.3$, $^2J_{\text{PP}} = 21.1$ Hz, 1P, P¹), 64.9 (dd, $^1J_{\text{PRh}} = 149.9$, $^2J_{\text{PP}} = 21.1$ Hz, 1P, P²).

X-Ray Measurements and Structure Determination of **8.** Single crystals of $\text{RhCl}_2(\eta^3\text{-C}_3\text{H}_5)(\text{SiNP})$ (**8**) were obtained by the slow diffusion of hexane into a CH_2Cl_2 solution of the compound. Crystal data, collected reflections, and parameters of the final refinement are reported in Table 3. Intensity data were collected using a Philips PW1100 diffractometer (FEBO system) with graphite-monochromated (Mo $\text{K}\alpha$) radiation, following the standard procedures. There were no significant fluctuations of intensities other than those expected from Poisson statistics. All intensities were corrected for Lorentz polarization and absorption.²⁰ The structures were solved by standard direct methods.²¹ All non-H atoms were located in the subsequent Fourier maps. Refinement was carried out by full-matrix least-squares procedures (based on F_o^2) using anisotropic temperature factors for all non-hydrogen atoms. The H atoms were placed in calculated positions with fixed, isotropic thermal parameters ($1.2U_{\text{equiv}}$) of the parent carbon atom. Calculations were performed with the SHELX-97 program²² implemented in the WinGX package.²³

Reaction of $\text{RhCl}_2(\eta^3\text{-C}_3\text{H}_5)(\text{SiNP})$ (8**) with CO.** In a NMR tube, $\text{RhCl}_2(\eta^3\text{-C}_3\text{H}_5)(\text{SiNP})$ (**8**, 10.7 mg, 12.5 μmol) was dissolved in C_6D_6 (0.4 mL). The resulting solution was saturated with CO and stirred under a CO atmosphere for 2 h. The mixture was analyzed via ^1H and ^{31}P NMR, showing the clean and quantitative formation of $\text{RhCl}(\text{CO})(\text{SiNP})$ (**5**) and 3-chloro-1-propene (confirmed by GC-MS).

Synthesis of $\text{Rh}(\text{Me})(\text{I})(\text{acac})(\text{SiNP})$ (10**).** A solution of MeI (15.6 μL , 2.28 g/mL, 0.251 mmol) in toluene was added to $\text{Rh}(\text{acac})(\text{SiNP})$ (**4**, 211 mg, 0.251 mmol) dissolved in toluene (15 mL). The mixture was allowed to stir at room temperature for 2 h. Then, all volatiles were removed and the residue crystallized from toluene/hexane

Scheme 9

(**10**, 155 mg, 63% yield). Found: C, 56.15; H, 5.22; N, 2.64. Calcd for $\text{C}_{46}\text{H}_{50}\text{IN}_2\text{O}_2\text{P}_2\text{RhSi}$ (982.74): C, 56.22; H, 5.13; N, 2.85. ^1H NMR (C_6D_6 , 298 K, δ_{C} from ^1H ^{13}C HSQC NMR, cf. Scheme 9 for labeling): δ 8.57 (br, 4H, PPh, C not observed), 7.91 (br, 4H, PPh, $\delta_{\text{C}} = 133.5$), 7.34 (dd, $J = 8.2, 1.8$; 2H, $\text{C}^2\text{H}^{\text{d}}$, $\delta_{\text{C}} = 131.7$), 7.17 (dd, $J = 8.2, 1.9, 2\text{H}$, $\text{C}^2\text{H}^{\text{u}}$, $\delta_{\text{C}} = 135.7$), 7.14 (6H, PPh, $\delta_{\text{C}} = 129.4, 126.4$), 7.10 (t, $^2J_{\text{HH}} = 7.3, 2\text{H}$, PPh, $\delta_{\text{C}} = 130.1$), 7.02 (br, 4H, PPh, $\delta_{\text{C}} = 125.6$), 6.72 (dd, $J = 8.2, 1.9, 2\text{H}$, $\text{C}^3\text{H}^{\text{d}}$, $\delta_{\text{C}} = 128.1$), 6.47 (dd, $J = 8.2, 1.9, 2\text{H}$, $\text{C}^3\text{H}^{\text{u}}$, $\delta_{\text{C}} = 129.1$), 5.63 (s, 1H, CH^{acac} , $\delta_{\text{C}} = 99.8$), 1.97 (s, 6H, Me^{acac} , $\delta_{\text{C}} = 27.7$), 1.94 (s, 6H, Me^{tol} , $\delta_{\text{C}} = 20.5$), 1.17 (s, 3H, SiMe^{u} , $\delta_{\text{C}} = 3.1$), 0.71 (q, $J = 2.2, 3\text{H}$, RhMe, $\delta_{\text{C}} = 32.3$, dt, $J = 23.0, 4.8$), 0.69 (s, 3H, SiMe^{d} , $\delta_{\text{C}} = 5.3$). δ_{C} (from ^{13}C NMR spectrum): 184.9 (CO), 139.1 (m, C^1), 135.8 (C^4), 134.0 (m, *ipso*-PPh). ^{31}P NMR (C_6D_6 , 298 K): δ 90.7 (d, $^1J_{\text{PRh}} = 143.9$).

^1H NMR (acetone- d_6 , 203 K, cf. Scheme 9 for labeling): δ 9.83 (br, 1H, o' -PPh^d, $\delta_{\text{C}} = 141.4$), 8.61 (br, 1H, o' -PPh^u, $\delta_{\text{C}} = 132.6$), 7.78 (t, $^3J_{\text{HH}} = 6.8$ Hz, 1H, m' -PPh^u, $\delta_{\text{C}} = 127.7$), 7.43–7.31 (2H, p -PPh^u, $\delta_{\text{C}} = 129.66$, + m' -PPh^d, $\delta_{\text{C}} = 125.5$), 7.28–7.18 (2H, p -PPh^d, $\delta_{\text{C}} = 130.2$, + $\text{C}^2\text{H}^{\text{u}}$, $\delta_{\text{C}} = 131.9$), 7.13 (t, $^3J_{\text{HH}} = 6.9$ Hz, 1H, m'' -PPh^u, $\delta_{\text{C}} = 126.0$), 6.95 (d, $^3J_{\text{HH}} = 7.4$ Hz, 1H, $\text{C}^3\text{H}^{\text{u}}$, $\delta_{\text{C}} = 128.4$), 6.64 (br, o'' -PPh^u, $\delta_{\text{C}} = 133.3$), 6.57 (t, $^3J_{\text{HH}} = 7.4$ Hz, 1H, m'' -PPh^d, $\delta_{\text{C}} = 125.3$), 6.53 (d, $^3J_{\text{HH}} = 8.5$ Hz, 1H, $\text{C}^3\text{H}^{\text{d}}$, $\delta_{\text{C}} = 128.4$), 6.32 (d, $^3J_{\text{HH}} = 8.2$ Hz, 1H, $\text{C}^2\text{H}^{\text{d}}$, $\delta_{\text{C}} = 134.8$), 6.04 (br, 1H, o'' -PPh^d, $\delta_{\text{C}} = 135.3$), 5.41 (s, 1H, CH^{acac} , $\delta_{\text{C}} = 99.1$), 2.05 (s, 6H, Me^{tol} , $\delta_{\text{C}} = 20.0$), 1.70 (s, 6H, Me^{acac} , $\delta_{\text{C}} = 27.1$), 0.43 (s, 3H, SiMe^{d} , $\delta_{\text{C}} = 1.5$), 0.41 (s, 3H, SiMe^{u} , $\delta_{\text{C}} = 4.4$), –0.08 (br, 3H, RhMe, $\delta_{\text{C}} = 32.5$). δ_{C} (from ^1H ^{13}C HSQC NMR): 184.1 (CO), 138.2 (C^1), 136.0 (C^4). ^{31}P NMR (acetone- d_6 , 203 K): δ 89.6 (d, $^1J_{\text{PRh}} = 143.3$ Hz).

Reaction of $\text{Rh}(\text{acac})(\text{SiNP})$ (4**) with 3-Chloro-1-propene.** 3-Chloro-1-propene (24.6 μL , 0.939 g/mL, 0.302 mmol) was added to a toluene solution (15 mL) of $\text{Rh}(\text{acac})(\text{SiNP})$ (**4**, 254 mg, 0.302 mmol). The mixture was allowed to stir at room temperature for 3 h. A portion of the liquid was analyzed by GC-MS, and the presence of 3-allylpentane-2,4-dione was observed along with traces (<5%) of 3,3-diallylpentane-2,4-dione. All of the volatiles were removed *in vacuo* and the sticky residue washed with hexane (2×5 mL), thus yielding a deep orange solid spectroscopically (^1H , ^{31}P) identified as $[\text{RhCl}(\text{SiNP})]_2$ (**2**, 208 mg, 89% yield). As a confirmation, when the reaction was carried out on a NMR-tube scale (12.0 mg of **4**, 1.2 μL of allylchloride), the clean formation of 3-allylpentane-2,4-dione and 3,3-diallylpentane-2,4-dione (traces) along with $[\text{RhCl}(\text{SiNP})]_2$ was observed.

When the reaction was carried out at 203 K, the intermediates $\text{RhCl}(\text{acac})(\eta^1\text{-C}_3\text{H}_5)(\text{SiNP})$ (**9a**) and $[\text{Rh}(\text{acac})(\eta^3\text{-C}_3\text{H}_5)(\text{SiNP})]\text{Cl}$ (**9b**) were detected and spectroscopically characterized (cf. Figure 3 for selected NMR data).

■ ASSOCIATED CONTENT

Supporting Information. Additional NMR data, details about the activation and thermodynamic parameters' determinations, and a CIF file. This material is available free of charge via the Internet at <http://pubs.acs.org>.

■ AUTHOR INFORMATION

Corresponding Author

*E-mail: passarel@unizar.es.

ACKNOWLEDGMENT

Funding was provided by MICINN (CTQ 2008-03860) and Fondazione G. Donegani—Accademia dei Lincei (G. Donegani Programme). V.P. thanks CSIC for the “I3P-Doctores” grant (2006-09).

REFERENCES

- (1) Gopalakrishnan, J. *Appl. Organomet. Chem.* **2009**, *23*, 291–318 and references therein.
- (2) Clarke, M. L.; Slawin, A. M. Z.; Woolins, J. D. *Phosphorus Sulfur Silicon Relat. Elem.* **2001**, *168–169*, 329–332.
- (3) Aucott, S. M.; Clarke, M. L.; Slawin, A. M. Z.; Woolins, J. D. *J. Chem. Soc., Dalton Trans.* **2001**, 972–976.
- (4) Gudat, D.; Daniels, L. M.; Verkade, J. G. *Organometallics* **1990**, *9*, 1464–1470.
- (5) Dowing, J. H.; Smith, M. B. In *Comprehensive Coordination Chemistry*, Clever, J. A., Meyer, T. J., Eds.; Elsevier Pergamon Press: Oxford, U.K., 2004; Vol. 1, pp 253–296.
- (6) Selected references are: Balakrishna, M. S.; Chandrasekaran, P.; George, P. P. *Coord. Chem., Rev.* **2003**, *241*, 87–117. Dahlenburg, L. *Coord. Chem. Rev.* **2005**, *249*, 2962–2992. Birkholz, M. N.; Freixa, Z.; Van Leeuwen, P. W. N. M. *Chem. Soc. Rev.* **2009**, *38*, 1099–1118. Zhang, X.; Chi, Y.; Tang, W. In *Comprehensive Organometallic Chemistry III*; Crabtree, R. H., Mingos, D. M. P., Eds.; Elsevier: Oxford, U.K., 2007; Vol. 10, p 1.
- (7) According to the Stokes–Einstein equation for spherical diffusing species [$D_X = (k_B T) / (6\pi\eta r_X)$], k_B is the Boltzmann constant, T is the temperature, and η is the viscosity of the solvent]. The diffusion coefficient (D_X) is inversely proportional to the hydrodynamic radius (r_X). If we consider two species (A and B), one (A) with a 2-fold hydrodynamic volume compared to the other (B), the ratio between the radii is $r_A/r_B = 2^{1/3} = 1.26$; therefore, $D_B/D_A = r_A/r_B = 1.26$.
- (8) Jardin, F. H. In *Encyclopedia of Inorganic Chemistry*, 2nd ed.; King, R. B., Ed.; John Wiley and Sons: New York, 2006; Vol. 7, pp 4693–4722.
- (9) 2006 cm^{-1} , for the dppe complex $\text{RhCl}(\text{CO})(\text{dppe})$. See: Lamb, G. W.; Law, D.; Slawin, A. M. Z.; Clarke, M. L. *Inorg. Chim. Acta* **2009**, *362*, 4263.
- (10) 2037 cm^{-1} , for $\text{RhCl}(\text{CO})(\text{P}_2)$, $\text{P}_2 = \text{bis}(3\text{-}(\text{diphenylphosphinooxy})\text{naphthalen-2-yl})\text{methane}$. See: Punji, B.; Mague, J. T.; Balakrishna, M. S. *Dalton Trans.* **2006**, 1322.
- (11) Serron, S.; Nolan, S. P.; Moloy, K. G. *Organometallics* **1996**, *15*, 4301–4306. Pribula, A. J.; Drago, R. S. *J. Am. Chem. Soc.* **1976**, *98*, 2784–2788.
- (12) The entropy error was estimated from the linear least-squares analysis without taking into account the error associated with each equilibrium constant measurement.
- (13) For instance, see $[\text{Rh}(\mu\text{-Cl})(\eta^3\text{-C}_3\text{H}_5)_2]_2$ (CCDC refcode ALYLRH01) and $[\text{Rh}_3(\mu^3\text{-tz})(\mu_2\text{-Cl})\text{Cl}(\eta^3\text{-C}_3\text{H}_5)_2(\text{CO})_4]$ (Htz = thiazole) (CCDC refcode COYYEU).
- (14) The structure of the azasilatrane complex $\text{PtCl}_2(\text{L})$, $\text{L} = \text{EtOSi}(\text{Ph}_2\text{PNCH}_2\text{CH}_2)_2(\text{HNCH}_2\text{CH}_2)\text{N}$, is highly disordered (cf. ref 4); therefore its comparison with **8** would be meaningless and has been omitted.
- (15) Dierkes, P.; Van Leeuwen, P. W. N. M. *J. Chem. Soc., Dalton Trans.* **1999**, 1519–1529.
- (16) The entropy error was estimated from the linear least-squares analysis (cf. Supporting Information) without taking into account the error associated with each rate constant measurement.
- (17) The ^{31}P NMR doublet at 90.7 ppm of **10** indicates a symmetric bidentate coordination of the SiNP ligand to the metal center. Furthermore, the smaller $^1J_{\text{PRh}}$ of **10** when compared with **4** is in agreement with the higher oxidation state of the metal center. The RhMe signals are observed as a pseudoquartet (^1H) and doublet of triplets (^{13}C) in agreement with the proposed *cis* arrangement of the CH_3 ligand with respect to both phosphorus atoms (cf. Experimental Section). The coordination sphere of the metal is completed by a symmetrically chelating acac ligand in the equatorial plane and the iodide in the remaining axial position. As a confirmation, the two SiMe_2 methyls are not equivalent, one facing RhMe and the other facing iodide. As far as the PPh_2 moieties are concerned, the ^1H NMR spectrum shows several broad signals indicative of a fluxional behavior, which reasonably could be the exchanging between the *up* and *down* semispace (cf. Experimental Section). Indeed, the ^1H NMR at 203 K shows well-resolved sharp resonances which could be assigned to two equivalent PPh_2 moieties, each containing two nonequivalent phenyl rings.
- (18) Wucker, B.; Moser, M.; Schumacher, S. A.; Rominger, F.; Kunz, D. *Angew. Chem., Int. Ed.* **2009**, *48*, 4417. Evans, P. A.; Nelson, J. D. *J. Am. Chem. Soc.* **1998**, *120*, 5581. Muraoka, T.; Matsuda, I.; Itoh, K.; Ueno, K. *Organometallics* **2007**, *26*, 387. Leahy, D. K.; Evans, P. A.; Rhodium(I)-catalyzed Allylic Substitution Reactions and their Applications to Target Directed Synthesis. In *Modern Rhodium-Catalyzed Reactions*; Evans, P. A., Ed.; Wiley-VCH: Weinheim, Germany, 2005; pp 191–214.
- (19) Stilbs, P. *Prog. Nucl. Magn. Reson. Spectrosc.* **1987**, *19*, 1–45. Price, W. S. *Concepts Magn. Reson.* **1997**, *9*, 299. Price, W. S. *Concepts Magn. Reson.* **1998**, *10*, 197. Johnson, C. S., Jr. *Prog. Nucl. Magn. Reson. Spectrosc.* **1999**, *34*, 203. Cohen, Y.; Avram, L.; Frish, L. *Angew. Chem.* **2005**, *117*, 524. Cohen, Y.; Avram, L.; Frish, L. *Angew. Chem., Int. Ed.* **2005**, *44*, 520. Pregosin, P. S.; Kumar, P. G. A.; Fernandez, I. *Chem. Rev.* **2005**, *105*, 2977. Macchioni, A.; Ciancaleoni, G.; Zuccaccia, C.; Zuccaccia, D. *Chem. Soc. Rev.* **2008**, *37*, 479.
- (20) North, A. T. C.; Philips, D. C.; Mathews, F. S. *Acta Crystallogr.* **1968**, *A24*, 351–359.
- (21) Burla, A. M. C.; Caliandro, R.; Camalli, M.; Carrozzini, B.; Cascarano, G. L.; De Caro, L.; Giacovazzo, C.; Polidori, G.; Spagna, R. *J. Appl. Crystallogr.* **2005**, *38*, 381–388.
- (22) Sheldrick, G. M. *SHELXL-97*; University of Göttingen: Göttingen, Germany, 1997.
- (23) Farrugia, L. J. *J. Appl. Crystallogr.* **1999**, *32*, 837–838.